Complex-Valued Spatial Filters for SSVEP-Based BCIs With Phase Coding

Owen Falzon*, *Student Member, IEEE*, Kenneth Camilleri, *Senior Member, IEEE*, and Joseph Muscat

Abstract—Brain–computer interface (BCI) systems based on steady-state visual evoked potentials (SSVEPs) have gained considerable popularity because of the robustness and high information transfer rate these can provide. Typical SSVEP setups make use of visual targets flashing at different frequencies, where a user's choice is determined from the SSVEPs elicited by the user gazing at a specific target. The range of stimulus frequencies available for such setups is limited by a variety of factors, including the strength of the evoked potentials as well as user comfort and safety with light stimuli flashing at those frequencies. One way to tackle this limitation is by introducing targets flickering at the same frequency but with different phases. In this paper, we propose the use of the analytic common spatial patterns (ACSPs) method to discriminate between phase coded SSVEP targets, and we demonstrate that the complex-valued spatial filters used for discrimination can exceed the performance of existing techniques. Furthermore, the ACSP method also yields a set of spatial patterns, separable into amplitude and phase components, that provide insight into the underlying brain activity.

Index Terms—Brain–computer interface (BCI), common spatial patterns (CSPs), electroencephalography (EEG), phase patterns, spatial filtering, steady-state visual evoked potential (SSVEP).

I. INTRODUCTION

DURING the last two decades there has been an increasing effort to develop mechanisms that can provide an individual with a means of communication and control to the outside world solely through brain activity [1], [2], be it for rehabilitation [3], [4] or gaming purposes [5], [6]. Noninvasive EEG electrodes are the preferred choice for most of these brain–computer interface (BCI) systems because they offer a high temporal resolution and constitute a relatively low cost solution compared to other recording modalities, with their main drawback being their limited spatial resolution.

Various neurophysiological phenomena have been considered for BCIs, with the most widely adopted including sensorimotor activity [7], P300 [8], and visual evoked potentials (VEPs) [2], [9]. In particular, BCI setups based on steady-state VEPs (SSVEPs) have received considerable attention because of the high information transfer rate and good reliability these can offer [10], [11].

Typical SSVEP-based BCI setups consist of visual targets flashing at different frequencies, where a user selects the target of interest by gazing at it. The SSVEP signals acquired from an individual's EEG are expected to exhibit spectral characteristics related to those of the target signal.

SSVEPs are also phase-locked to the target stimulus [12]. This characteristic can be used to increase the number of choices for a user by adding targets at the same frequency but with varying phases. Alternatively, an SSVEP-based BCI setup may be rendered more robust by determining frequencies that elicit the best SSVEP response for a given user and introducing targets with phase shifts at those frequencies.

Most SSVEP setups, including those that consider phase information, adopt an EEG channel pair based on prior neurophysiological knowledge [13], [14] or based on a specific preprocessing step [9], [15]. Others consider a multichannel scenario and make use of spatial filtering methods to optimally combine the information from various channels and improve the performance of the BCI system [16], [17].

In this paper, we propose the use of the analytic common spatial patterns (ACSPs) algorithm that we recently proposed in [18] as a combined spatial filtering and feature extraction technique to identify a user's selection when presented with flickering visual targets exhibiting phase differences. Experiments on an offline BCI setup were conducted to demonstrate the characteristics of the ACSP technique and compare its performance to a number of other techniques that are commonly adopted in SSVEP-based BCI setups.

This paper proceeds as follows: in the next section, the background for SSVEP-based BCI setups, particularly for those setups that use phase coding, is provided, together with details on the use of spatial filtering for SSVEP-based BCIs. This is followed by the theory of the ACSP technique in Section III. In Section IV, a description of the experimental protocol adopted for this study is presented including a brief description of the other methods considered for the comparative performance analysis. Section V contains the classification accuracies obtained from the various techniques. The performance outcome and characteristics of the various methods are then discussed in detail in Section VI.

II. BACKGROUND ON PHASE CODED SSVEP-BASED BCIs

Most SSVEP-based BCI systems consist of a setup where a user is presented with a number of visual targets, typically

consisting of LEDs, or square or checkerboard patterns on an LCD, flickering within the 5-40 Hz range [5], [9], [11], [17]. When the user's gaze is focused on one of the targets, the occipital and parietal regions of the brain exhibit neural activity at the stimulus frequency [9]. Thus, by determining the prominent frequency components in the recorded EEG signals, the target of interest can be identified.

For such SSVEP setups, the number of targets used is limited by the number of frequencies that can elicit a strong response in the EEG activity of an individual while allowing comfortable and safe use of the system for extended periods of time [11].

A. Phase in SSVEP-Based BCI Setups

Considering that SSVEPs are phase-locked to the visual stimulus [12], [19], it is possible to identify visual targets flickering at the same frequency but with variations in phase. This phase-locking characteristic allows phase coding in SSVEP setups, leading to two main advantages: phase coding can increase the number of targets available, and can compensate for a reduction in the set of selected frequencies (to cater for user comfort and safety).

SSVEP setups that make use of phase coding generally extract the phase information from the SSVEP signals either from Fourier coefficients [15], [20], [21], [22] or by computing the Hilbert transform [23], [24]. This phase information is subsequently used to detect the target of interest.

To our knowledge, the first account of phase information being used for target identification in an SSVEP setup is that by Cilliers and van der Kouwe [25] where a setup with four stimulus LEDs exhibiting $90°$ phase steps was used and target detection was carried out by cross correlation of the EEG with previously recorded EEG activity. More recently, Kluge and Hartmann [13], [20] considered a phase-based SSVEP setup to reduce the probability of error in an SSVEP-based BCI, and demonstrated that incorporating phase information can improve the system's performance compared to a setup that extracts only amplitude information from the acquired EEG data. Subsequently, the use of phase in SSVEP-based BCIs was adopted in various setups in order to increase the number of targets available and improve BCI performance [15], [21], [22], [24].

B. Spatial Filtering for SSVEP-Based BCI Setups

Most SSVEP-based BCI setups, including those that utilize phase coding, only consider two EEG channels for data acquisition and processing [14], [20], [22], [25]. This reduces hardware and computational requirements, but comes at a cost in terms of performance. The considered pair of channels are typically selected based on the prior knowledge that SSVEPs are generated in the occipital and parietal regions of the brain. However, since SSVEP topography is subject specific [9], [19], the selection of two electrodes based solely on prior neurophysiological knowledge is unlikely to give an optimal level of performance.

An alternative is to select the most appropriate EEG channel pair based on the outcome of a preprocessing step, such as ICA [15], [26]. A subject-specific optimal channel pair is thus determined after initial testing on a larger electrode set.

An approach that may lead to a significant improvement in the system's performance involves retaining a greater number of EEG channels and using spatial filters to combine these optimally for discrimination. These spatial filters are often designed to maximize the SSVEP components with respect to background nonstimulus activity [16], [17], [27], [28]. Spatial filtering methods used in SSVEP setups to enhance the distinction between EEG data from stimulus and nonstimulus conditions include the maximum contrast combination (MCC) method [16], the minimum energy combination (MEC) method [16], and the common spatial patterns (CSPs) method [17].

The MCC method involves the computation of a weight matrix such that the energy in the SSVEP frequencies is maximized while that in the EEG activity not related to the SSVEP component is minimized [23], [24]. On the other hand, the MEC spatial filtering approach attempts to cancel out EEG activity that is not related to the SSVEP response by minimizing the energy in the undesirable EEG signals [16]. The CSP method [29] has been adopted in several BCI setups and is typically used to distinguish conditions involving attenuation and enhancement of EEG rhythms such as sensorimotor activity [30]. In the only cases we are aware of where CSP was employed in relation to SSVEPs [17], [28], the method was used to enhance the SSVEP signal by maximizing the signal-to-noise ratio of the visual-evoked response against the nonstimulus condition. After the application of one of these spatial filtering stages to enhance the SSVEP signal, the features for discriminating between the various flashing targets are obtained through a separate feature extraction stage [24].

In this study, we apply the ACSP algorithm to directly distinguish the recorded data corresponding to the various flickering targets. Therefore, rather than applying the spatial filtering method to discriminate EEG data from the stimulus and nonstimulus conditions, and subsequently extracting features for discrimination, the spatial filters are optimized to directly distinguish the SSVEP data for the different targets. Through this approach the spatial filtering and feature extraction stages are effectively combined in a single step as will be detailed in the following section.

III. PROPOSED METHOD

In its basic form, the ACSP method involves the discrimination of EEG data corresponding to two different target conditions by maximizing the expression

$$\max_{w \in \mathbb{C}^N} \frac{w^* \mathbf{C_1} w}{w^* \mathbf{C_2} w} \qquad (1)$$

where N is the number of channels considered, $\mathbf{C_1}$ and $\mathbf{C_2}$ represent the covariance matrices for two classes of data, w is the spatial filter to determine, and $(\cdot)^*$ denotes the conjugate transpose. Unlike the CSP method, for ACSP the EEG signals are transformed into their analytic representation using the Hilbert transform. Thus, a complex representation of the data is obtained where amplitude and phase information are considered explicitly [18]. This renders the algorithm particularly useful for setups where the differences in the phase information are

crucial for discrimination as in the case of phase coded SSVEP setups.

Complex-valued covariance matrices are computed from the analytic signals and a simultaneous diagonalization procedure is carried out on the covariance matrices from the two classes. This results in a set of complex-valued spatial filters that optimally discriminate between the data for the targets considered by maximizing the variance of one class while minimizing the variance of the other.

A. Analytic Signal Representation

A real signal can be converted into its analytic representation by using the Hilbert transform. The complex form that results allows for amplitude and phase information incorporated in the signal to be considered explicitly in the analysis.

For a real signal $x(t)$, the analytic representation $z(t)$ is given by

$$z(t) = x(t) + j\hat{x}(t) = A(t)e^{j\phi(t)} \tag{2}$$

where $\hat{x}(t)$ is the Hilbert transform of $x(t)$ [31]. $A(t)$ and $\phi(t)$ represent the instantaneous amplitude and the instantaneous phase, respectively, and are obtained from

$$A(t) = \sqrt{x^2(t) + \hat{x}^2(t)} \quad \text{and} \quad \phi(t) = \arctan\left(\frac{\hat{x}(t)}{x(t)}\right). \tag{3}$$

After converting the original real-valued signals into their complex-valued counterparts, a covariance matrix is computed for each trial. The covariance matrices from a set of training trials for each condition are averaged and the resulting matrices are used as inputs for the joint diagonalization step. A joint diagonalization procedure similar to the conventional CSP method follows with the difference that for the ACSP algorithm this is adapted to handle complex-valued matrices.

B. Joint Diagonalization of Complex-Valued Matrices

Let $\mathbf{X}_1, \mathbf{X}_2 \in \mathbb{R}^{N \times T}$ represent real-valued band-pass filtered EEG data for two conditions, where N is the number of EEG channels and T is the number of samples per channel. The corresponding analytic counterparts are given by $\mathbf{Z}_1$ and $\mathbf{Z}_2 \in \mathbb{C}^{N \times T}$.

The covariance matrix of $\mathbf{Z}_1$ is given by

$$\mathbf{C}_1 = \mathrm{E}\left[(\mathbf{Z}_1 - \mathrm{E}[\mathbf{Z}_1])(\mathbf{Z}_1 - \mathrm{E}[\mathbf{Z}_1])^*\right] \tag{4}$$

where $\mathrm{E}[\cdot]$ represents the expectation operator. The same procedure can be applied for $\mathbf{Z}_2$ to obtain $\mathbf{C}_2$. Thus, $\mathbf{C}_1$ and $\mathbf{C}_2$ constitute a pair of $N \times N$ Hermitian positive semidefinite matrices, with real-valued elements along the main diagonal and generally complex-valued off-diagonal elements. The main idea behind the ACSP method (as for the CSP procedure) is to maximize the expression in (1). This can be achieved through the joint diagonalization of the covariance matrices of the multichannel data for the two conditions [32]. Now, for two matrices to be simultaneously diagonalizable they must be commutable [33]. This is not necessarily the case for $\mathbf{C}_1$ and $\mathbf{C}_2$ so these two matrices have to be transformed such that they are commutable.

Here, we develop the ACSP using a novel mathematical theory based on the inverse square-root matrix of $\mathbf{C}_c := \mathbf{C}_1 + \mathbf{C}_2$, which is given by

$$\mathbf{C}_c^{-\frac{1}{2}} = \mathbf{L}_c \mathbf{\Lambda}_c^{-\frac{1}{2}} \mathbf{L}_c^* \tag{5}$$

where the columns of $\mathbf{L}_c$ are the eigenvectors corresponding to the real-valued eigenvalues in the diagonal matrix $\mathbf{\Lambda}_c$. $\mathbf{C}_c$ can be whitened by $\mathbf{C}_c^{-\frac{1}{2}}$ such that

$$\begin{aligned} \mathbf{I} &= \mathbf{C}_c^{-\frac{1}{2}} \mathbf{C}_c \mathbf{C}_c^{-\frac{1}{2}} \\ &= \mathbf{C}_c^{-\frac{1}{2}} \mathbf{C}_1 \mathbf{C}_c^{-\frac{1}{2}} + \mathbf{C}_c^{-\frac{1}{2}} \mathbf{C}_2 \mathbf{C}_c^{-\frac{1}{2}} \\ &:= \mathbf{S}_1 + \mathbf{S}_2. \end{aligned} \tag{6}$$

Now for $\mathbf{S}_1$ and $\mathbf{S}_2$ to be commutable and simultaneously diagonalizable it has to be shown that $\mathbf{S}_1\mathbf{S}_2 = \mathbf{S}_2\mathbf{S}_1$. From (6), this is the same as proving that

$$\mathbf{C}_1 \mathbf{C}_c^{-1} \mathbf{C}_2 = \mathbf{C}_2 \mathbf{C}_c^{-1} \mathbf{C}_1. \tag{7}$$

This can be proved by expanding $\mathbf{C}_c := \mathbf{C}_1 + \mathbf{C}_2$ such that

$$\mathbf{C}_c \mathbf{C}_c^{-1} \mathbf{C}_1 = \mathbf{C}_1 \mathbf{C}_c^{-1} \mathbf{C}_1 + \mathbf{C}_2 \mathbf{C}_c^{-1} \mathbf{C}_1$$

$$\mathbf{C}_1 - \mathbf{C}_1 \mathbf{C}_c^{-1} \mathbf{C}_1 = \mathbf{C}_2 \mathbf{C}_c^{-1} \mathbf{C}_1$$

$$\mathbf{C}_1 - \mathbf{C}_1 \mathbf{C}_c^{-1} (\mathbf{C}_c - \mathbf{C}_2) = \mathbf{C}_2 \mathbf{C}_c^{-1} \mathbf{C}_1$$

$$\mathbf{C}_1 \mathbf{C}_c^{-1} \mathbf{C}_2 = \mathbf{C}_2 \mathbf{C}_c^{-1} \mathbf{C}_1. \tag{8}$$

If (6) is premultiplied and postmultiplied by $\mathbf{U}_1^*$ and $\mathbf{U}_1$, respectively, where $\mathbf{U}_1$ is the matrix of eigenvectors of $\mathbf{S}_1$, then

$$\mathbf{I} = \mathbf{U}_1^* \mathbf{S}_1 \mathbf{U}_1 + \mathbf{U}_1^* \mathbf{S}_2 \mathbf{U}_1 = \mathbf{\Lambda}_1 + \mathbf{U}_1^* \mathbf{S}_2 \mathbf{U}_1 \tag{9}$$

and

$$\mathbf{U}_1^* \mathbf{S}_2 \mathbf{U}_1 = \mathbf{I} - \mathbf{\Lambda}_1 = \mathbf{\Lambda}_2. \tag{10}$$

Therefore, the corresponding real-valued diagonal elements in $\mathbf{\Lambda}_1$ and $\mathbf{\Lambda}_2$ add up to 1 and are ordered such that when the diagonal elements in $\mathbf{\Lambda}_1$ decrease, those in $\mathbf{\Lambda}_2$ increase (or vice versa).

A projection matrix $\mathbf{W}$ can thus be obtained from

$$\mathbf{W} = \mathbf{U}_1^* \mathbf{C}_c^{-\frac{1}{2}} \tag{11}$$

where the rows of $\mathbf{W}$ correspond to a set of spatial filters that maximize the variance for one class of data and minimize the variance for the other class.

Generally, once the spatial filters for discriminating between two classes are determined from a set of training trials, only the first and last m spatial filters are retained as these are expected to be the most discriminative [34].

The features for discrimination can then be obtained by considering the extreme diagonal elements of $\mathbf{W}\mathbf{C}_z\mathbf{W}^*$, where $\mathbf{C}_z$ is the covariance of a given trial $\mathbf{Z}$. The features for classification f_z are then obtained from the retained diagonal elements d_z where

$$f_z = \log\left(\frac{d_z}{\sum_{i=1}^{2m} d_z}\right). \tag{12}$$

In the aforementioned expression the logarithm of the diagonal elements is computed to normalize the feature distribution [29], [34].

In addition to the spatial filters $\mathbf{W}$, a set of spatial patterns can be derived from the columns of $\mathbf{A}$, where $\mathbf{A} = \mathbf{W}^{-1}$. Now, given that data from a trial $\mathbf{Z}$ can be projected to yield a set of discriminative components $\mathbf{Y}$, where

$$\mathbf{Y} = \mathbf{WZ} \tag{13}$$

the spatial patterns $\mathbf{A}$ can be used to reproject those components that are most significant for discrimination as scalp maps. The reprojected scalp signals $\tilde{\mathbf{Z}}$ can thus be obtained from

$$\tilde{\mathbf{Z}} = \tilde{\mathbf{A}}\tilde{\mathbf{Y}} \tag{14}$$

where $\tilde{\mathbf{Y}}$ constitutes those components that are most significant for discrimination and $\tilde{\mathbf{A}}$ are the associated spatial patterns. Thus, if considered cautiously, these spatial patterns may give useful neurophysiological insight onto the discriminating brain activity related to a given set of tasks [30].

The principal difference between the CSP and ACSP methods thus lies in the complex covariance matrices used for the latter technique. The complex-valued elements of the covariance matrices can capture and represent additional information on the interchannel interactions that exist in the data when compared to their real-valued counterparts since the complex components can be separated into explicit amplitude and phase components. The complex-valued spatial filters and spatial patterns obtained from the joint diagonalization process can then lead to a better classification of data as well as an improved representation of the discriminating characteristics in the data. In fact, in circumstances where phase differences play a significant role in the data, the spatial patterns from the CSP method may lead to misleading interpretations of the underlying activity in the considered data [18]. On the other hand, the ACSP method can handle phase variations between channels in a more effective manner, leading to a more accurate representation. The improvement in the representation obtained from the ACSP method with respect to the CSP technique is demonstrated through the following toy example.

C. Toy Example

A simulation consisting of simple sinusoidal signals generated for three scalp locations is shown in Fig. 1. The signals at each location have a particular magnitude and phase value denoted by $|\mathrm{A}|$ and ϕ, respectively, that may vary for the two conditions. The amplitudes of the signals are normalized with respect to the signal at location A. This signal is also taken as the zero phase reference and the phases of the other signals are measured with respect to it. The principal difference between the two classes of data lies in the $60°$ phase shift of the signals from locations B and C in Class 2 with respect to those from Class 1. Such a situation resembles a phase coded SSVEP scenario with a $60°$ phase difference between two visual targets that elicit an SSVEP response at locations B and C. By considering the phases of the signals from B and C with respect to a common
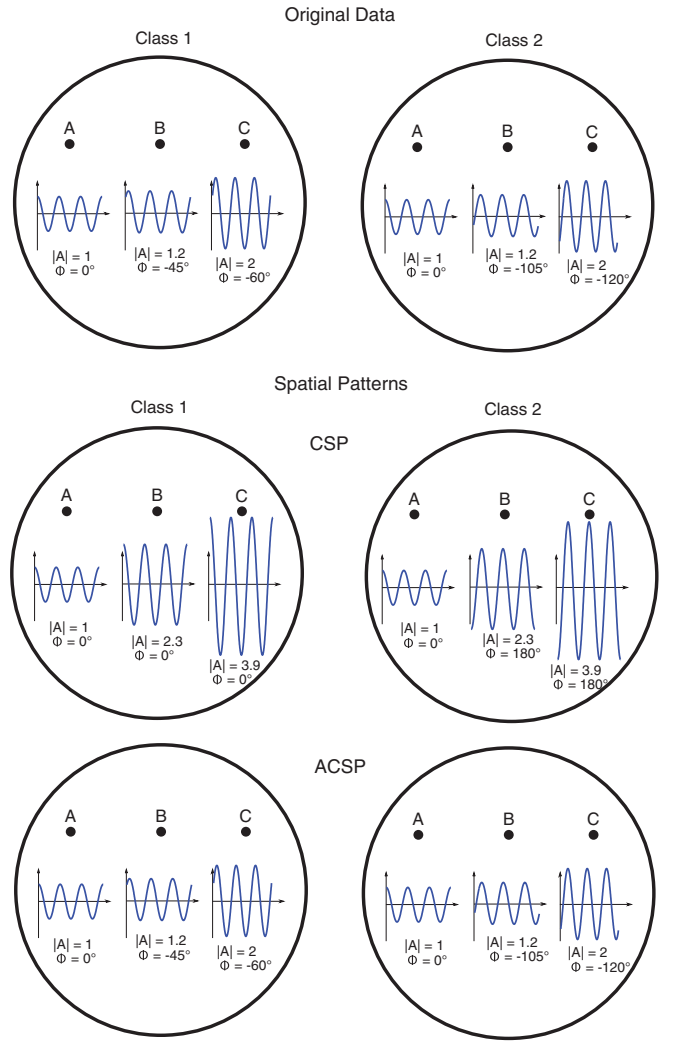

Fig. 1. Toy example with simulated signals from three scalp locations. The original signals for two classes of data together with their magnitude ($|\mathrm{A}|$) and phase (ϕ) values are shown in the top figure. The spatial patterns that result from the CSP and ACSP methods are shown in the bottom representations. The spatial patterns from the ACSP method give a more realistic picture of the underlying activity in the original data when compared to those obtained from the CSP method. The improved representation attained from the ACSP method is attributed to the representation of the data in the complex domain that allows for the explicit consideration of amplitude and phase characteristics in the data.

reference signal for the two classes (at location A in this case), the phase lag associated with the two targets can be determined.

The CSP and ACSP methods were applied to the data from the two classes and a set of spatial filters and spatial patterns were obtained from each method. The spatial patterns give a representation of the underlying characteristics in the data that are significant for discrimination and these are shown through the values of the most discriminative spatial patterns and the corresponding scalp reprojections, $\tilde{\mathbf{Z}}$ obtained from these. However, while the spatial patterns from the CSP technique give real-valued representations that can only show phase relationships between the spatial locations that are in phase or $180°$ out of phase (in the case of negative values), the complex-valued spatial patterns from the ACSP method can be separated into explicit magnitude and phase components. This has the advantage of
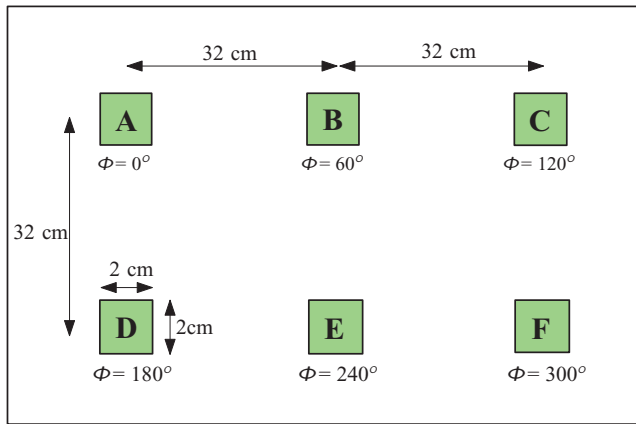
Fig. 2. Representation of the panel with the six target LED sets, all flashing at 7 Hz but with phase values of 0°, 60°, 120°, 180°, 240°, and 300° for targets A, B, C, D, E, and F, respectively. Subjects were seated about 75 cm away from the panel with each target subtending an angle of approximately 1.5°
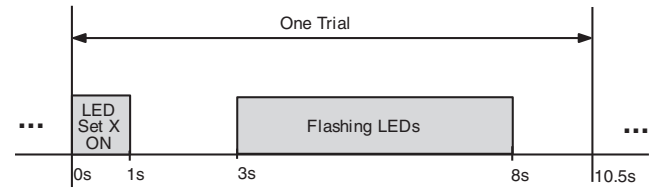

Fig. 3. Sequence of events for each trial. A 2 s interval from 0.5 until 2.5 s from the onset of the flashing LEDs was considered for further processing.

allowing a representation of the whole range of phase values as opposed to the limited outcome of the CSP technique.

From the amplitude and phase values of the spatial pattern coefficients resulting from the CSP and ACSP methods shown in Fig. 1, it is evident that the restricted representation of phase relationships with the CSP method can lead to misleading interpretations. Apart from an inadequate representation of phase relationships, inaccurate signal magnitudes further compromise the interpretation of the resulting patterns. On the other hand, the spatial patterns obtained from the ACSP approach give a faithful representation of the underlying amplitude and phase characteristics in the original classes of data, thereby leading to the outcome of the ACSP method being more reliable than that from the conventional CSP approach.

In the next section, the experimental protocol used to test the ACSP method on actual EEG data from an SSVEP setup is described and the performance of the technique is compared to that of the CSP approach and a number of other methods used in SSVEP-based BCI setups.

IV. EXPERIMENTAL PARADIGM

An SSVEP-based BCI setup with phase coded targets was used to evaluate the performance of the ACSP algorithm and compare its outcome with respect to the CSP method and the other spatial filtering and feature extraction methods mentioned in Section II. In this section, the experimental setup and data acquisition procedures are presented, followed by a description of the methods used for the analysis.

A. Experimental Setup and Data Acquisition

The experimental setup consisted of a typical SSVEP setup where a subject makes a selection by directing his or her attention to one of a number of flashing targets [11], [15], [20], [24]. Six visual targets consisting of green LEDs flashing at 7 Hz with phase differences in steps of 60° (i.e., phases of 0°, 60°, 120°, 180°, 240°, and 300°) were utilized. A representation of the target panel is shown in Fig. 2. Subjects were seated at a dis-

tance of approximately 75 cm from the panel, with each flashing target thus covering an angle of approximately 1.5° in the user's visual field. Although higher frequencies are typically preferred for SSVEP-based BCI systems, the aim of this study is to assess the performance of the ACSP technique with respect to other methods given the same data, and therefore the actual stimulus frequency used is not of major relevance in this case.

Six subjects gave their informed consent to participate in this study approved by the University of Malta Research Ethics Committee. All participants had normal or corrected-to-normal vision. For each subject 72 trials were recorded, 12 for each target. Each trial lasted 10.5 s starting with an interval of 1 s during which the target LED set was lit up constantly. This served to indicate to the users the target toward which the subjects had to direct their attention during that trial. Subsequently, all the target LEDs were switched OFF for a period of 2 s. The participants then had to look toward the indicated target while all the LED sets flickered for 5 s. A rest period of 2.5 s followed, during which all the LEDs were OFF again, and the whole process was repeated for the 72 trials. Fig. 3 illustrates the sequence of events making up a trial. The participants were asked to avoid eye blinks and movements during the 5 s interval while the LEDs were flashing.

For the processing and analysis stages a 2 s interval starting from 0.5 until 2.5 s after the onset of the flashing LEDs was extracted from the trials.

Data were acquired using 32 active EEG electrodes at a sampling rate of 1200 Hz from a g.tec g.USBamp amplifier. Eventually, six channels in the occipital and parietal regions, namely O1, Oz, O2 PO5, POz, and PO6, were considered for further analysis. The reference electrode was connected to the left earlobe and the ground electrode at AFz. The 72 recorded trials were divided into tenfolds for a stratified tenfold cross-validation procedure, where the trials from nine of the folds were used to estimate the parameters for each of the implemented algorithms while the remaining fold was used for testing. For every given method, an average classification accuracy was estimated by averaging the classification accuracies for the ten test folds obtained through the cross-validation iterations.

B. CSP and ACSP Implementation

The only cases where, to our knowledge, the CSP method was used in conjunction with SSVEPs was to maximize the signal-to-noise ratio of the visual-evoked responses against the nonstimulus condition [17], [28]. However, the method has never been used to distinguish between data related to phase-shifted targets from SSVEP-based setups. In this study, instead

of using the spatial filters from the CSP and ACSP methods to enhance the SSVEP signals with respect to background EEG activity, the spatial filters are designed to directly discriminate between the different phase coded targets. For an adequate comparison of the CSP and ACSP methods, the same procedure was adopted for the two methods.

Spectral filtering was carried out on the EEG signals using a predefined bandpass FIR least squares filter of order 300, a bandwidth of 1.5 Hz and a preselected center frequency at f_c. The recorded EEG data were filtered separately with three such filters differing in their center frequency. The first filter was centered at $f_c = 7$ Hz corresponding to the SSVEP fundamental frequency, the second filter was centered at $f_c = 14$ Hz being the second harmonic of the SSVEP fundamental, and the third filter was centered at $f_c = 21$ Hz being the third harmonic. By having these three datasets any improvements that may be achieved by using features from additional SSVEP harmonics could be investigated [35]. Specifically, the experiments were first carried out on data obtained from the filter centered at the fundamental frequency; the number of harmonics n_h considered was equal to 1. The same experiments were also carried out for $n_h = 2$, where features extracted from data filtered at the fundamental frequency were combined with features extracted from the data filtered at the second harmonic. Similarly for $n_h = 3$, features were extracted from the three sets of data and combined.

The CSP and ACSP methods operate on the covariance matrices of the data. However, the computation of the covariance matrices leads to a loss of the temporal element and thus a loss of the relative phase difference between the visual targets. Since, the SSVEP activity in the brain may be expected to be similar for all the visual targets, the covariance matrices associated with the various targets would also be expected to be practically identical unless a phase reference signal is included. Therefore, a sinusoidal signal synchronized with the first LED set (Target A) was recorded as the $0°$-phase reference signal and appended as an additional channel to the EEG data to create an augmented dataset for the CSP and ACSP methods. This augmented data representation then yields covariance matrices that are discriminable for the different targets.

In their standard form, the CSP and ACSP methods are designed to work with two classes of data. However, since in this study there are six target conditions, a multiclass extension of the techniques is adopted. Following one approach in [36], spatial filters were determined for each pairwise combination of classes based on the training dataset. For each pairwise combination of classes, features were extracted as specified in (12) using the first and last spatial filters as is typical for the CSP method [34]. The computation of these filters for the ACSP method requires twice the number of parameters due to the complex-valued elements of the filters. However, the dimensionality of the classification problem is the same for both methods, that is, one value for each spatial filter as described in Section III. An LDA classifier was then trained on features extracted from the training dataset and applied to the test set for each pairwise combination of classes. Majority voting was then used to assign the class label to the test trial.

The use of more complex classifiers such as SVMs did not yield any particular improvement in classification accuracy when compared to LDA. In this paper, the results from the CSP method are mainly intended to highlight the improvement of the ACSP method over the standard CSP implementation when dealing with classes of data where phase information is relevant for discrimination given the exact same input data and procedural conditions.

C. Implementation of the Other Methods

In addition to the CSP algorithm, a number of methods typically used in SSVEP-based BCI setups were also implemented and their performance was compared to that obtained from the ACSP technique. A brief description of these methods follows. As for the CSP and ACSP methods, a stratified tenfold cross-validation approach was adopted in all the cases. Specifically, any procedures for spatial filters parameter estimation, channel selection, and classifier training were carried out using data from the nine training folds. The remaining data fold was then used to determine the classification performance of the methods. An LDA classifier was adopted for all the methods.

1) *FFT (Oz-POz)*: in several SSVEP setups a channel pair from the occipital or parietal region is often selected to acquire the SSVEP signal. The relevant phase information is then extracted from the Fourier coefficients associated with the frequency of interest [13], [20], [25], [37]. For this purpose, one of the methods considered in this analysis utilizes the Oz-POz channel pair (found to give close to optimal performance in some cases [15]) to represent a channel choice based purely on prior neurophysiological knowledge. For each trial, a feature extraction approach similar to that of Jia *et al.* [15] was adopted. Specifically, the Fourier coefficients associated with the frequencies of interest were computed, and the real and complex part of the coefficients (without normalization in order to retain both the amplitude and phase information in the features) were used as features. The use of other feature extraction methods such as the Hilbert transform as in [24] did not yield any improvement in classification accuracy.

2) *FFT (best)*: considering that the preselected Oz-POz pair may not be the best performing channel pair for a given subject, a procedure was carried out to consider the best possible results that can be obtained from a channel pair selection method. The best performing subject-specific channel pair was determined through ninefold cross-validation carried out on the nine training folds within the tenfold cross-validation procedure described earlier for each possible channel pair. Features for that selected channel pair were then extracted from the test fold in the tenfold cross-validation procedure. The features were obtained from the Fourier coefficients as for the FFT (Oz-POz) approach.

3) *MCC*: the MCC method [16] for spatial filtering has been considered in some SSVEP setups that include phase shifts in the targets [23], [24], in order to enhance the SSVEP signal. A set of spatial filters from the training data were

determined, and the filters that produce the greatest energy in the SSVEP subspace with respect to the energy in the rest of the signal were retained as detailed in Friman *et al.* [16]. The EEG data were transformed with the selected MCC spatial filters, and features were extracted using the Fourier coefficients of the transformed signals as for the FFT (Oz-POz) method. This was found to give a better result than the phase differences obtained using the Hilbert transform and was thus the approach adopted in our implementation.

4) *MEC*: the MEC method combines the EEG signals from various electrodes in order to remove the undesired non-SSVEP components in the data. To our knowledge this spatial filtering method has never been considered in an SSVEP setup with phase coding. We therefore apply the MEC method on phase coded SSVEP setups for the first time in this study to provide a more comprehensive analysis. The filters are determined using the training data, and a number of filters are retained according to a preselected threshold as is detailed in [16]. Features from the Fourier coefficients were extracted and classified using the same procedure as described for the MCC approach.

In the following section, the results obtained from the implemented techniques are presented and compared to the outcome obtained from the ACSP method.

V. COMPARATIVE PERFORMANCE RESULTS

The classification accuracies obtained from the ACSP approach, the standard CSP implementation and the other methods mentioned in the previous section are provided in Table I. For each case, the classification accuracy obtained when considering up to three harmonics is presented, together with the mean performance across all subjects for each method. Results from the best performing techniques for each subject (for the different number of harmonics n_h considered) and the best overall results across all subjects are shown in bold.

A. ACSP Versus CSP

The results for the ACSP and CSP methods in Table I demonstrate that the use of the ACSP method yields a considerable improvement in classification accuracy over the CSP technique. Averaging across all subjects, the ACSP method yields a statistically significant improvement ($p < 0.05$) of approximately 10% (for any number of harmonics considered) over the standard CSP technique. This confirms our hypothesis that the ACSP is expected to outperform CSP when phase constitutes an important characteristic in the class conditioned data.

For the SSVEP-based BCI setup in this study, a set of spatial filters and spatial patterns were determined for each possible pairwise combination of target classes. For the computed spatial patterns, the spatial amplitude maps were normalized, and the spatial phase patterns are represented with respect to the phase coefficient of the $0°$-phase reference signal. Therefore, the phase coefficient of the $0°$-phase reference channel is represented by $0°$ for each class and all other channel phase coefficients are with respect to this reference phase. In Fig. 4, the spatial pat-

TABLE I
PERCENTAGE OF CORRECTLY CLASSIFIED TRIALS
(n_h: NO. OF HARMONICS CONSIDERED)

Classification Accuracy (%)							
Subject	n_h	Method
		FFT (best)	FFT (Oz-POz)	MCC	MEC	CSP	ACSP
S1	1	83	83	79	**88**	64	76
	2	**89**	**89**	84	84	67	86
	3	**93**	91	86	90	72	92
S2	1	63	29	64	**69**	65	65
	2	82	51	89	84	73	**93**
	3	84	52	**96**	86	78	94
S3	1	90	90	94	**96**	95	**96**
	2	99	99	99	97	97	**100**
	3	**99**	**99**	96	94	96	**99**
S4	1	80	21	**82**	69	35	**82**
	2	90	24	**93**	81	60	88
	3	89	29	**92**	76	76	86
S5	1	82	75	64	63	79	**88**
	2	94	92	91	89	94	**96**
	3	96	94	96	90	96	**97**
S6	1	**96**	**96**	94	93	92	**96**
	2	**96**	**96**	92	94	95	95
	3	**96**	**96**	92	88	92	**96**
Mean	1	82	66	80	80	72	**84**
	2	92	75	91	88	81	**93**
	3	93	77	93	87	85	**94**

terns obtained from the CSP and the ACSP methods for the EEG data for the first harmonic from subject S6 are shown. The patterns displayed for each target were obtained from each of the pairwise class combinations with respect to Target A, and the patterns for Target A itself were those that resulted when this was considered in combination with Target B. The spatial patterns that result for the other pairwise class combinations are consistent with those shown in Fig. 4 and are thus not included here. The spatial amplitude patterns from the ACSP method indicate a high activity at channel location POz across all classes. In the case of the spatial phase maps, the coefficients for the spatial locations, taken with respect to the reference phase signal, exhibit a progressive step of approximately $60°$ across the target classes as expected from the SSVEP setup used for the experiment. For instance, considering channel POz, the difference in the spatial phase pattern coefficient for this channel for Targets B, C, D, E, and F with respect to Target A approximates the expected phase differences of $60°$, $120°$, $180°$, $240°$ and $300°$, respectively. This contrasts with the spatial patterns from the CSP approach where the representation of the data is limited to an amplitude map thereby restricting the representation of phase variations to be in phase or $180°$ out of phase in the case of negative spatial pattern values. Furthermore, the spatial patterns from the CSP method show differences in the amplitude maps for the different classes while the amplitude maps from the ACSP method for the various targets show a consistent activity. These issues are discussed further in Section VI.

B. ACSP Versus Other Techniques Used in Phase-Based SSVEPs

Considering the classification accuracy of the ACSP method with respect to the other methods (see Table I), the ACSP
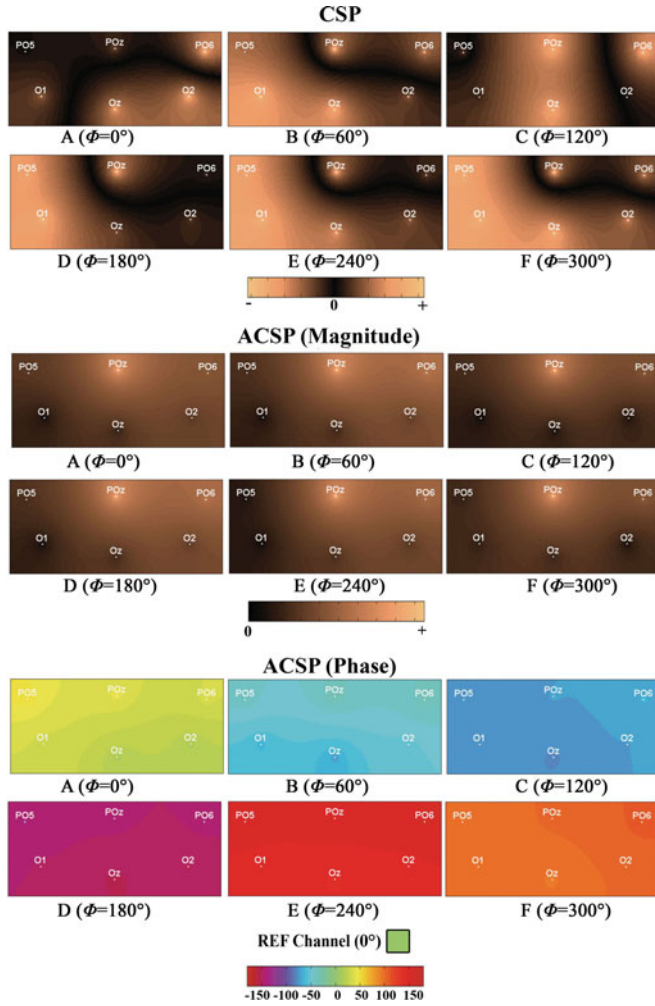
Fig. 4. Representation of the spatial patterns obtained when considering the first harmonic for Subject S6. The spatial patterns obtained from the CSP and ACSP methods for each pairwise class combination with respect to Target A are shown. The complex-valued spatial patterns from the ACSP method are separated into amplitude and phase components where the phase values shown are obtained with respect to the phase coefficient associated with the reference sinusoidal signal. For the ACSP method, the amplitude patterns show considerable similarity across the targets as expected, and the phase differences between the phase patterns for the different conditions are closely related to the incremental 60° difference exhibited by the stimulus visual targets. On the other hand, the real-valued spatial patterns obtained from the conventional CSP method can yield no information on phase differences in the EEG data or with respect to the reference phase signal coefficient, except for a 180° phase shift. Furthermore, the spatial patterns obtained from the CSP method are not always consistent across targets, confirming that the amplitude map may lead to inadequate interpretations.

technique yields the best overall accuracy for any combination of harmonics for Subjects S3 and S5. It is also the best technique or one of the best faring techniques for most harmonic combinations for the other subjects. On average, the ACSP technique is the best performing method for any number of harmonics considered, with a classification accuracy of 84%, 93%, and 94% for $n_h = 1$, 2, and 3, respectively.

Through *t*-tests, it was confirmed that the ACSP method performs significantly ($p < 0.05$) better than the FFT (Oz-POz) and CSP approaches. There is no statistically significant difference in performance between ACSP and MCC, MEC, or FFT (best),

all of which have comparable performances. However, ACSP yields spatial phase maps that may provide useful information regarding the class data that are not yielded by MCC, MEC or FFT (best).

VI. DISCUSSION

The results presented in the previous section show that the ACSP method is one of the best performing techniques for all subjects. When compared to the conventional CSP technique, the proposed ACSP approach gave a statistically significant improvement in classification accuracy. The factors that lead to this improvement are considered next, followed by a discussion comparing the performance of the ACSP method to that of the other techniques.

A. ACSP Versus CSP

Although for the CSP method, the real-valued elements of the covariance matrix of the augmented data set do not explicitly represent channel phase relationships, the value of these elements may be implicitly affected by the channel phase relationships. Therefore, the covariance matrices of the augmented dataset obtained for the different target classes may exhibit interclass differences thereby allowing the CSP method the possibility to discriminate between the classes. However, as we have shown in [18], the complex-valued covariance matrices used in the ACSP method will always capture the phase relationships in an explicit manner whereas the CSP may at times fail. Consequently, CSP features may not be able to discriminate as consistently as ACSP features.

1) Advantages of Complex-Valued Spatial Filters: the complex-valued covariance matrices obtained from the analytic signals capture the amplitude and phase relationships in the data in an explicit manner as opposed to the covariance matrices computed for the original data. For the latter, the interchannel interactions are represented by a single value that incorporates both the influence of amplitude and phase relationships. The computed complex-valued covariance matrices for the ACSP method thus yield a set of complex-valued spatial filters that can also be separated into magnitude and phase components. These filters can lead to a significant advantage: in addition to an optimally weighted summation of signals as for the conventional CSP approach, a phase shift is also applied to each signal from the various scalp locations that can further aid discrimination.

In our earlier work [18], we have shown that when two datasets are distinguishable solely through the phase interactions between the signals, there may be circumstances where the spatial filters that result from the CSP method turn out to be completely ineffective in separating the two classes of data, while the ACSP technique still succeeds in capturing these dissimilarities in phase and in maximizing the difference between the variances of the two classes. Therefore, while for classification purposes both the ACSP and CSP methods yield the same number of features, the complex-valued spatial filters from ACSP have a greater discriminative ability than those from the CSP method.

2) Advantages of Complex-Valued Spatial Patterns: The complex-valued spatial patterns from the ACSP method, $\mathbf{A} = \mathbf{W}^{-1}$, can be represented by separate amplitude and phase maps and can provide a more accurate representation of the underlying neuronal activity than the CSP method.

The main difference between the target classes for the phase coded SSVEP setup is expected to consist of the incremental $60°$ step for the SSVEP signals phase-locked to Targets A to F. Therefore, one would expect the most discriminative spatial patterns to capture this phase difference while the amplitude maps are expected to show a relatively constant pattern across the classes. These patterns of activity are in fact observable in the spatial patterns obtained from the ACSP method as shown in Fig. 4. On the other hand, the spatial patterns obtained from the CSP method can only give amplitude information, which is, however, influenced by both amplitude and phase interactions in the data. In fact, the spatial patterns for the CSP method in Fig. 4 could lead to the erroneous interpretation that SSVEPs are evoked at different spatial locations for the different targets. Clearly, this should not be the case and further confirms that for the standard CSP method phase differences in the data may lead to distortions in the resulting amplitude map as also shown in the earlier toy example. With the complex-valued spatial patterns from the ACSP approach, these issues are effectively resolved through a separate representation of amplitude and phase components that yield a more accurate representation of the underlying activity.

Interestingly, from the spatial phase maps, it can also be noted that there is a slight phase variation along the posterior to the anterior direction of the scalp. These may be associated with travelling wave properties that are sometimes observed during the stimulation of SSVEPs [12]. Such gradual phase variations that characterize travelling waves cannot be appropriately represented with the CSP spatial patterns. On the contrary, the ACSP approach can capture these phase changes along the scalp thereby allowing for a better examination of the ongoing activity. However, since the scope of this study mainly involves a comparison of the proposed ACSP method with other techniques used in phase coded SSVEP-based BCIs, this issue is not considered in further depth in this study.

B. ACSP Versus Other Techniques Used in Phase-Based SSVEPs

The results in Table I indicate that the heuristic selection of a channel pair as in the case of the Oz-POz channel pair considered in the FFT (Oz-POz) method, may in some cases be a sufficiently good choice, as in the case of Subjects S1, S3, S5, and S6, where the channel pair is in fact the best or gives a classification accuracy close to the best channel pair. However, this is not guaranteed to be the optimal choice as is evident from the relatively poor results obtained for the other subjects. This variation in the outcomes can be attributed to the effect of topographic variations for SSVEP responses across subjects [9], differences in electrode placement, and other physiological factors such as tissue characteristics that may vary across individuals.

Therefore, the consideration of a greater number of channels is expected to yield more reliable results.

The use of multiple channels is therefore generally expected to yield a better performance than an *a priori* selected pair. Additionally, the use of spatial filtering techniques does not require a search for the best performing channel pairs when compared to methods such as FFT (best). Considering the methods that employed a spatial filtering approach, the ACSP method gave the best classification accuracy.

One important difference between the ACSP approach and the MCC and MEC approaches is that in the former the filters are optimized to discriminate directly between the classes of data considered. On the other hand, the MCC and MEC methods are typically employed to enhance the SSVEP signal with respect to background EEG data. Phase extraction was subsequently carried out as an independent step. The ACSP method effectively combines the two stages and yields a set of spatial filters that take into account the phase differences between the data channels (in this case consisting of the EEG channels and the additional reference phase signal).

Similar to the CSP approach, the spatial filters from the MEC and MCC techniques result in filters limited to real-valued coefficients, thus limiting their interpretation when compared to the complex-valued spatial filters and spatial patterns obtained from the ACSP technique.

VII. Conclusion

In this paper, we have proposed the use of an extension of the conventional CSP approach, namely the ACSP method, and showed how this can be successfully applied to a phase-based SSVEP application. Through this study, we have shown that the ACSP method can yield a significant improvement over the conventional CSP approach when considering classes of data that involve class-dependent phase differences. The ACSP approach was also compared to a number of methods that have been utilized or that are applicable to SSVEP-based BCIs incorporating phase coding. The results obtained show that the ACSP technique is amongst the top performing methods. In addition to the high classification rate obtained, a set of spatial patterns can be extracted from the ACSP method that can give a more accurate representation of the underlying discriminant brain activity than those obtained from the conventional CSP method. We have demonstrated that on average the classification accuracy from the ACSP technique exceeds that of existing methods for phase coded SSVEP setups, making it a very attractive candidate for target identification in such setups.

References

[1] G. Dornhege, J. d. R. Millán, T. Hinterberger, D. J. McFarland, and K.-R. Müller, *Toward Brain-Computer Interfacing.* Cambridge, MA: The MIT Press, 2007.

[2] A. Bashashati, M. Fatourechi, R. K. Ward, and G. E. Birch, "A survey of signal processing algorithms in brain-computer interfaces based on electrical brain signals," *J. Neural Eng.*, vol. 4, no. 2, pp. R32–R57, Jun. 2007.

[3] G. R. Müller-Putz and G. Pfurtscheller, "Control of an electrical prosthesis with an SSVEP-based BCI," *IEEE Trans. Biomed. Eng.*, vol. 55, no. 1, pp. 361–364, Jan. 2008.

[4] G. Pfurtscheller, G. R. Müller-Putz, R. Scherer, and C. Neuper, "Rehabilitation with brain-computer interface systems," *IEEE Comput.*, vol. 41, no. 10, pp. 58–65, Oct. 2008.

[5] E. C. Lalor, S. P. Kelly, C. Finucane, R. Burke, R. Smith, R. B. Reilly, and G. McDarby, "Steady-state VEP-based brain-computer interface control in an immersive 3D gaming environment," *EURASIP J. Adv. Signal Process.*, vol. 2005, pp. 3156–3164, 2005.

[6] R. Krepki, B. Blankertz, G. Curio, and K.-R. Müller, "The Berlin brain-computer interface (BBCI)—Towards a new communication channel for online control in gaming applications," *Multimedia Tools Applicat.*, vol. 33, pp. 73–90, Apr. 2007.

[7] J. R. Wolpaw, D. J. McFarland, T. M. Vaughan, and G. Schalk, "The Wadsworth center brain-computer interface (BCI) research and development program," *IEEE Trans. Neural Syst. Rehabil. Eng.*, vol. 11, no. 2, pp. 204–207, Jun. 2003.

[8] E. Donchin, K. Spencer, and R. Wijesinghe, "The mental prosthesis: Assessing the speed of a P300-based brain-computer interface," *IEEE Trans. Rehabil. Eng.*, vol. 8, no. 2, pp. 174–179, Jun. 2000.

[9] F.-B. Vialatte, M. Maurice, J. Dauwels, and A. Cichocki, "Steady-state visually evoked potentials: Focus on essential paradigms and future perspectives," *Prog. Neurobiol.*, vol. 90, no. 4, pp. 418–438, 2010.

[10] G. Bin, X. Gao, Y. Wang, B. Hong, and S. Gao, "Research frontier: VEP-based brain-computer interfaces: Time, frequency, and code modulations," *IEEE Comput. Intell. Mag.*, vol. 4, no. 4, pp. 22–26, Nov. 2009.

[11] D. Zhu, J. Bieger, G. G. Molina, and R. M. Aarts, "A survey of stimulation methods used in SSVEP-based BCIs," *Comput. Intell. Neurosci.*, vol. 2010, pp. 1–12, Jan. 2010.

[12] G. Burkitt, R. Silberstein, P. Cadusch, and A. Wood, "Steady-state visual evoked potentials and travelling waves," *Clin. Neurophysiol.*, vol. 111, no. 2, pp. 246–258, Feb. 2000.

[13] M. Hartmann and T. Kluge, "Phase coherent detection of steady-state evoked potentials: Theory and performance analysis," in *Proc. 3rd Int. IEEE/EMBS Conf. Neural Eng.*, May 2007, pp. 179–183.

[14] A. Luo and T. J. Sullivan, "A user-friendly SSVEP-based brain-computer interface using a time-domain classifier," *J. Neural Eng.*, vol. 7, no. 2, pp. 1–10, Mar. 2010.

[15] C. Jia, X. Gao, B. Hong, and S. Gao, "Frequency and phase mixed coding in SSVEP-based brain-computer interface," *IEEE Trans. Biomed. Eng.*, vol. 58, no. 1, pp. 200–206, Jan. 2011.

[16] O. Friman, I. Volosyak, and A. Gräser, "Multiple channel detection of steady-state visual evoked potentials for brain-computer interfaces," *IEEE Trans. Biomed. Eng.*, vol. 54, no. 4, pp. 742–750, Apr. 2007.

[17] S. Parini, L. Maggi, A. C. Turconi, and G. Andreoni, "A robust and self-paced BCI system based on a four class SSVEP paradigm: Algorithms and protocols for a high-transfer-rate direct brain communication," *Comput. Intell. Neurosci.*, vol. 2009, pp. 1–11, Jan. 2009.

[18] O. Falzon, K. P. Camilleri, and J. Muscat, "Complex-valued spatial filters for task discrimination," in *Proc. Annu. Int. Conf. IEEE Eng. Med. Biology Soc.*, Sep. 2010, pp. 4707–4710.

[19] S. T. Morgan, J. C. Hansen, and S. A. Hillyard, "Selective attention to stimulus location modulates the steady-state visual evoked potential," *Proc. Nat. Acad. Sci. USA*, vol. 93, no. 10, pp. 4770–4774, May 1996.

[20] T. Kluge and M. Hartmann, "Phase coherent detection of steady-state evoked potentials: Experimental results and application to brain-computer interfaces," in *Proc. 3rd Int. IEEE/EMBS Conf. Neural Eng.*, May 2007, pp. 425–429.

[21] C. M. Wong, B. Wang, F. Wan, P. U. Mak, P. I. Mak, and M. I. Vai, "An improved phase-tagged stimuli generation method in steady-state visual evoked potential based brain-computer interface," in *Proc. 3rd Int. Conf. Biomed. Eng. Informat.*, 2010, vol. 2, pp. 745–749.

[22] M. A. Lopez-Gordo, A. Prieto, F. Pelayo, and C. Morillas, "Use of phase in brain-computer interfaces based on steady-state visual evoked potentials," *Neural Process. Lett.*, vol. 32, pp. 1–9, Aug. 2010.

[23] D. Zhu, G. Molina, V. Mihajlovic, and R. Aarts, "Phase synchrony analysis for SSVEP-based BCIs," in *Proc. 2nd Int. Conf. Comput. Eng. Technol.*, 2010, vol. 2, pp. 329–333.

[24] G. G. Molina, D. Zhu, and S. Abtahi, "Phase detection in a visual-evoked-potential based brain computer interface," in *Proc. 18th Eur. Signal Process. Conf.*, 2010, pp. 949–953.

[25] P. Cilliers and A. van der Kouwe, "A system for VEP detection and stimulus phase discrimination," in *Proc. 15th Southern Biomed. Eng. Conf.*, Mar. 1996, pp. 77–80.

[26] Y. Wang, R. Wang, X. Gao, B. Hong, and S. Gao, "A practical VEP-based brain-computer interface," *IEEE Trans. Neural Syst. Rehabilit. Eng.*, vol. 14, no. 2, pp. 234–240, 2006.

[27] G. G. Molina and V. Mihajlovic, "Spatial filters to detect steady-state visual evoked potentials elicited by high frequency stimulation: BCI application," *Biomed. Eng.*, vol. 55, no. 3, pp. 173–182, 2010.

[28] G. Garcia-Molina and D. Zhu, "Optimal spatial filtering for the steady state visual evoked potential: BCI application," in *Proc. 5th Int. IEEE/EMBS Conf. Neural Eng.*, May 2011, pp. 156–160.

[29] J. Müller-Gerking, G. Pfurtscheller, and H. Flyvbjerg, "Designing optimal spatial filters for single-trial EEG classification in a movement task," *Clin. Neurophysiology*, vol. 110, no. 5, pp. 787–798, 1999.

[30] B. Blankertz, R. Tomioka, S. Lemm, M. Kawanabe, and K.-R. Müller, "Optimizing spatial filters for robust EEG single-trial analysis," *IEEE Signal Process. Mag.*, vol. 25, no. 1, pp. 41–56, Jan. 2008.

[31] L. Cohen, *Time-Frequency Analysis*. Englewood Cliffs, NJ: Prentice Hall, 1995, ch. 2, pp. 30–36.

[32] G. H. Golub and C. F. Van Loan, *Matrix Computations*, 3rd ed. Baltimore, MD: Johns Hopkins Univ. Press, 1996, ch. 8, pp. 461–463.

[33] R. A. Horn and C. R. Johnson, *Matrix Analysis*. New York, NY: Cambridge Univ. Press, 1990, ch. 1, pp. 49–54.

[34] H. Ramoser, J. Müller-Gerking, and G. Pfurtscheller, "Optimal spatial filtering of single trial EEG during imagined hand movement," *IEEE Trans. Biomed. Eng.*, vol. 8, no. 4, pp. 441–446, Dec. 2000.

[35] G. R. Müller-Putz, R. Scherer, C. Brauneis, and G. Pfurtscheller, "Steady-state visual evoked potential (SSVEP)-based communication: Impact of harmonic frequency components," *J. Neural Eng.*, vol. 2, no. 4, pp. 123–130, Dec. 2005.

[36] G. Dornhege, B. Blankertz, G. Curio, and K.-R. Müller, "Increase information transfer rates in BCI by CSP extension to multi-class," in *Advances in Neural Information Processing Systems*. vol. 16, Cambridge, MA: MIT Press, 2004, pp. 733–740.

[37] M. Lopez-Gordo, F. Pelayo, and A. Prieto, "A high performance SSVEP-BCI without gazing," in *Proc. Int. Joint Conf. Neural Networks*, 2010, pp. 1–5.

Owen Falzon (S'05) received the B.Eng. (Hons) degree in electrical engineering from the University of Malta, Msida, Malta, in 2006, and is currently working toward the Ph.D. degree on EEG signal processing applied to brain–computer interfaces at the same university.

He is an Assistant Lecturer with the Centre for Biomedical Cybernetics, University of Malta. His research interests include EEG signal analysis, brain–computer interfaces, and biomedical signal and image processing.

Kenneth P. Camilleri (SM'11) received the B.Elec.Eng. (Hons) degree in electrical engineering from the University of Malta, Msida, Malta, and received the M.Sc. degree in signal processing and machine intelligence and the Ph.D. degree in image processing and pattern recognition, in 1994 and 1999, respectively, both from the University of Surrey, Guildford, U.K. He is currently the Director of the Centre for Biomedical Cybernetics, University of Malta. His research interests include image texture analysis and segmentation, sketch and scribble image understanding and interpretation, thermal image processing, biomedical engineering and EEG signal analysis applied to the diagnosis of brain diseases and to brain–computer interfacing.

Joseph Muscat received the B.A. degree from Oxford University, Oxford, U.K., and the Ph.D. degree from Princeton University, Princeton, NJ.

He is a Lecturer at the Department of Mathematics, University of Malta, Msida, Malta. His research interests include differential equations and functional analysis, and their applications to biomedical engineering and bioinformatics.

Dr. Muscat is a member of the American Mathematical Society.